ICIC Express Letters
Volume **15**, Number **1**, January **2021**

 ISSN 1881-803X
pp. **37–42**

GENERATION OF MOIRE-LIKE IMAGES FROM RGB-D IMAGES

Ryousuke Takaki and Toru Hiraoka

Department of Information Systems
University of Nagasaki
1-1-1, Manabino, Nagayo-chou, Nishisonogi-gun, Nagasaki-ken 851-2195, Japan
{ MC220002; hiraoka }@sun.ac.jp

Received May 2020; accepted August 2020

Abstract. *A non-photorealistic rendering method has been proposed to generate moire-like images from photographic images using bilateral filter and unsharp mask. In recent years, stereo cameras mounted on smartphones have appeared, and it will be more accessible to obtain RGB-D images with RGB values and the depth in the future. Therefore, we develop a method for generating moire-like images from RGB-D images. As this time, the depth is incorporated into bilateral filter. As a result, it is possible to generate moire-like patterns having a texture different from that of the related art, thereby expanding the range of use according to the user's preference. We visually confirm moire-like images generated by the proposed method through experiments using RGB-D images obtained by the stereo camera.*
Keywords: Moire-like image, Depth, Distortion, Bilateral filter, Unsharp mask

1. **Introduction.** Bilateral filter [1, 2] that performs smoothing and preserves the edges of images has recently attracted attention, and has been used in a wide range of fields such as image processing [3, 4, 5] and computer graphics [6, 7]. It is known that a process of bilateral filter produces a staircasing effect [8, 9] of stepwise changes in shading. When bilateral filter is applied, a pseudo-contour line is generated due to the staircasing effect, so [8] has been conducted to eliminate the pseudo-contour line. On the other hand, a non-photorealistic rendering method has been proposed that generates moire-like images [10, 11] from photographic images by using unsharp mask to emphasize the pseudo-contour line. Moire-like images are a type of op art expressed by superimposing moire-like patterns on photographic images. A method [12] to move moire-like patterns and a method [13] to generate moire-like patterns at high speed have also been proposed.

In recent years, with the emergence of smartphones equipped with a stereo camera and the ability to obtain the depth, we develop a method for generating moire-like images from RGB-D images with RGB values and the depth. By using the depth, the types of expressions of moire-like images are increased, and moire-like images can be selected according to the user's preference and usage scene. The proposed method extends the conventional method [10, 11] by adding the depth to bilateral filter. As a result, moire-like patterns having different textures are generated between moire-like images of the proposed and conventional methods, and moire-like images of the proposed method are expressed in more distorted moire-like patterns than moire-like images of the conventional method. To verify the effectiveness of the proposed method, we performed experiments using RGB-D images taken with the stereo camera, and visually confirmed the change of moire-like images generated by changing the value of a parameter newly added to the proposed method. In addition, we visually compared moire-like images of the proposed and conventional methods.

DOI: 10.24507/icicel.15.01.37

This paper is organized as follows: the second section describes the proposed method for generating moire-like images from RGB-D images, the third section shows experimental results and reveals the effectiveness of the proposed method, and the conclusion of this paper is given in the fourth section.

2. **Proposed Method.** The proposed method is executed in two steps: the first step is to process using bilateral filter embedded the depth, and the second step is to process using unsharp mask. A flow chart of the proposed method is shown in Figure 1.

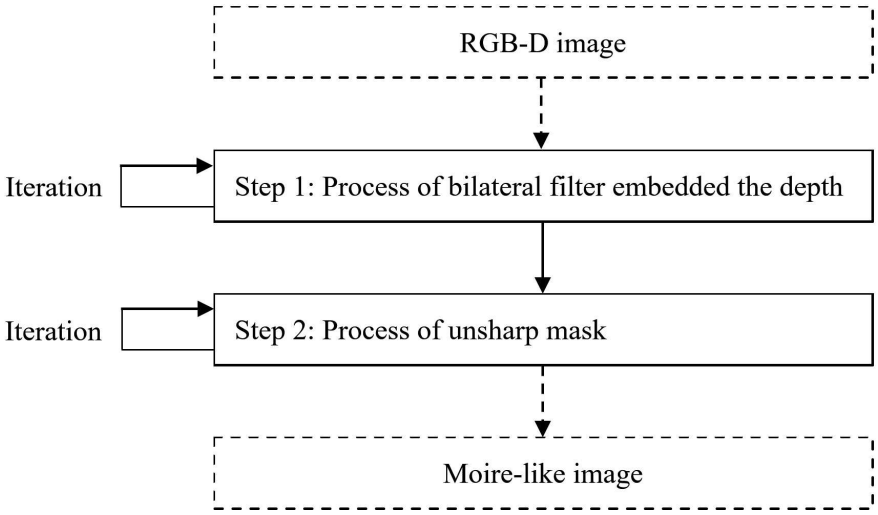

FIGURE 1. Flow chart of the proposed method

Details of the procedure in Figure 1 are explained below.

Step 0: The input pixel values (R, G, B) and the depth for spatial coordinates (i, j) of an RGB-D image are defined as $f_{R,i,j}$, $f_{G,i,j}$, $f_{B,i,j}$, and $f_{D,i,j}$, respectively. The pixel values $f_{R,i,j}$, $f_{G,i,j}$, and $f_{B,i,j}$ have value of U gradation from 0 to $U-1$, and the depth $f_{D,i,j}$ is stored in cm. Then, the pixel values of the image at the t-th iteration number are defined as $f^{(t)}_{R,i,j}$, $f^{(t)}_{G,i,j}$, and $f^{(t)}_{B,i,j}$, where $f^{(0)}_{R,i,j} = f_{R,i,j}$, $f^{(0)}_{G,i,j} = f_{G,i,j}$, and $f^{(0)}_{B,i,j} = f_{B,i,j}$.

Step 1: The output pixel values $f^{(t)}_{R,i,j}$, $f^{(t)}_{G,i,j}$, and $f^{(t)}_{B,i,j}$ in bilateral filter embedded the depth are calculated by the following equations.

$$f^{(t)}_{R,i,j} = \frac{\sum_{k=i-W}^{i+W}\sum_{l=j-W}^{j+W} e^{-\alpha\left((i-k)^2+(j-l)^2\right)-\beta\left(f^{(t-1)}_{R,i,j}-f^{(t-1)}_{R,k,l}\right)^2-\gamma(f_{D,i,j}-f_{D,k,l})^2} f^{(t-1)}_{R,k,l}}{\sum_{k=i-W}^{i+W}\sum_{l=j-W}^{j+W} e^{-\alpha\left((i-k)^2+(j-l)^2\right)-\beta\left(f^{(t-1)}_{R,i,j}-f^{(t-1)}_{R,k,l}\right)^2-\gamma(f_{D,i,j}-f_{D,k,l})^2}} \tag{1}$$

$$f^{(t)}_{G,i,j} = \frac{\sum_{k=i-W}^{i+W}\sum_{l=j-W}^{j+W} e^{-\alpha\left((i-k)^2+(j-l)^2\right)-\beta\left(f^{(t-1)}_{G,i,j}-f^{(t-1)}_{G,k,l}\right)^2-\gamma(f_{D,i,j}-f_{D,k,l})^2} f^{(t-1)}_{G,k,l}}{\sum_{k=i-W}^{i+W}\sum_{l=j-W}^{j+W} e^{-\alpha\left((i-k)^2+(j-l)^2\right)-\beta\left(f^{(t-1)}_{G,i,j}-f^{(t-1)}_{G,k,l}\right)^2-\gamma(f_{D,i,j}-f_{D,k,l})^2}} \tag{2}$$

$$f^{(t)}_{B,i,j} = \frac{\sum_{k=i-W}^{i+W}\sum_{l=j-W}^{j+W} e^{-\alpha\left((i-k)^2+(j-l)^2\right)-\beta\left(f^{(t-1)}_{B,i,j}-f^{(t-1)}_{B,k,l}\right)^2-\gamma(f_{D,i,j}-f_{D,k,l})^2} f^{(t-1)}_{B,k,l}}{\sum_{k=i-W}^{i+W}\sum_{l=j-W}^{j+W} e^{-\alpha\left((i-k)^2+(j-l)^2\right)-\beta\left(f^{(t-1)}_{B,i,j}-f^{(t-1)}_{B,k,l}\right)^2-\gamma(f_{D,i,j}-f_{D,k,l})^2}} \tag{3}$$

where W is the window size, α, β, and γ are positive constants, and k and l are the positions in the window. In Equations (1), (2), and (3), the term of $-\gamma(f_{D,i,j}-f_{D,k,l})^2$ is added to the coefficient of exponential function in the proposed method. The larger the value of γ is, the more different moire-like patterns from the conventional method

are generated. As the value of γ is 0, the same moire-like patterns as the conventional method are generated. The process of Step 1 is repeated T_1 times.

Step 2: The pixel values $f_{R,i,j}^{(T_1)}$, $f_{G,i,j}^{(T_1)}$, and $f_{B,i,j}^{(T_1)}$ are defined as $g_{R,i,j}^{(0)}$, $g_{G,i,j}^{(0)}$, and $g_{B,i,j}^{(0)}$, respectively. The output pixel values $g_{R,i,j}^{(t)}$, $g_{G,i,j}^{(t)}$, and $g_{B,i,j}^{(t)}$ in unsharp mask using bilateral filter are calculated by the following equations.

$$g_{R,i,j}^{(t)} = 2g_{R,i,j}^{(t-1)} - \frac{\sum_{k=i-W}^{i+W}\sum_{l=j-W}^{j+W} e^{-\alpha\left((i-k)^2+(j-l)^2\right)-\beta\left(g_{R,i,j}^{(t-1)}-g_{R,k,l}^{(t-1)}\right)^2} g_{R,k,l}^{(t-1)}}{\sum_{k=i-W}^{i+W}\sum_{l=j-W}^{j+W} e^{-\alpha\left((i-k)^2+(j-l)^2\right)-\beta\left(g_{R,i,j}^{(t-1)}-g_{R,k,l}^{(t-1)}\right)^2}} \tag{4}$$

$$g_{G,i,j}^{(t)} = 2g_{G,i,j}^{(t-1)} - \frac{\sum_{k=i-W}^{i+W}\sum_{l=j-W}^{j+W} e^{-\alpha\left((i-k)^2+(j-l)^2\right)-\beta\left(g_{G,i,j}^{(t-1)}-g_{G,k,l}^{(t-1)}\right)^2} g_{G,k,l}^{(t-1)}}{\sum_{k=i-W}^{i+W}\sum_{l=j-W}^{j+W} e^{-\alpha\left((i-k)^2+(j-l)^2\right)-\beta\left(g_{G,i,j}^{(t-1)}-g_{G,k,l}^{(t-1)}\right)^2}} \tag{5}$$

$$g_{B,i,j}^{(t)} = 2g_{B,i,j}^{(t-1)} - \frac{\sum_{k=i-W}^{i+W}\sum_{l=j-W}^{j+W} e^{-\alpha\left((i-k)^2+(j-l)^2\right)-\beta\left(g_{B,i,j}^{(t-1)}-g_{B,k,l}^{(t-1)}\right)^2} g_{B,k,l}^{(t-1)}}{\sum_{k=i-W}^{i+W}\sum_{l=j-W}^{j+W} e^{-\alpha\left((i-k)^2+(j-l)^2\right)-\beta\left(g_{B,i,j}^{(t-1)}-g_{B,k,l}^{(t-1)}\right)^2}} \tag{6}$$

In case $g_{R,i,j}^{(t)}$, $g_{G,i,j}^{(t)}$, and $g_{B,i,j}^{(t)}$ are less than 0, then $g_{R,i,j}^{(t)}$, $g_{G,i,j}^{(t)}$, and $g_{B,i,j}^{(t)}$ must be set to 0, respectively. In case $g_{R,i,j}^{(t)}$, $g_{G,i,j}^{(t)}$, and $g_{B,i,j}^{(t)}$ are greater than $U-1$, then $g_{R,i,j}^{(t)}$, $g_{G,i,j}^{(t)}$, and $g_{B,i,j}^{(t)}$ must be set to $U-1$, respectively. The process of Step 2 is repeated T_2 times, and an image composed of the pixel values $g_{R,i,j}^{(T_2)}$, $g_{G,i,j}^{(T_2)}$, and $g_{B,i,j}^{(T_2)}$ is the moire-like image.

3. **Experiments.** We conducted two experiments. The first experiment was to visually examine the changing moire-like patterns by changing the value of the parameter γ newly added by the proposed method. The second experiment visually compared moire-like patterns of the proposed and conventional methods.

RGB-D images were obtained using ZED stereo camera. In the following experiments, two RGB-D images shown in Figure 2 and Figure 3 were used. Figure 2 shows two people in the vicinity, and Figure 3 shows two people in the distance. The left sides of Figure 2 and Figure 3 are RGB images, and the right sides of Figure 2 and Figure 3 are depth images. In depth images, the brighter the region in depth images, the deeper the depth. Two RGB-D images used in the experiments were $1280 * 720$ pixels and 256 gradation.

In reference to [10, 11], the values of the parameters α, β, W, T_1, and T_2 used in all experiments were set to 0.01, 0.01, 20, 10, and 20, respectively. The smaller the value of the parameter α, the larger the spacing between moire-like patterns. The smaller the value of the parameter β, the less areas where moire-like patterns do not occur and moire-like

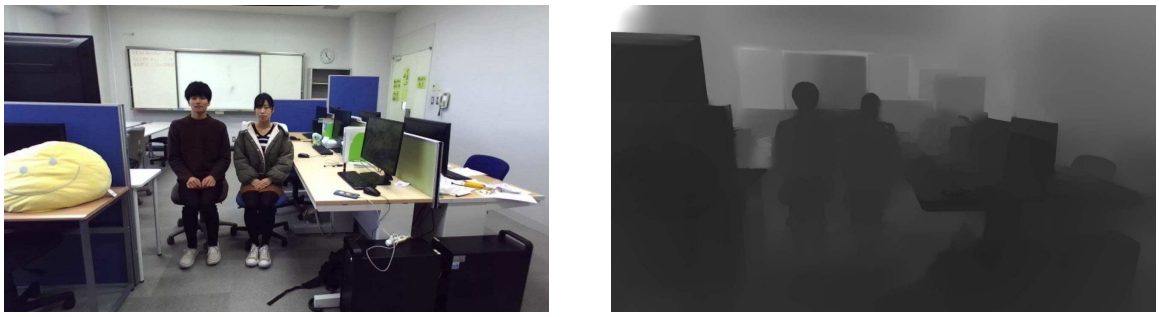

(a) RGB image (b) Depth image

FIGURE 2. RGB-D image (Near view)

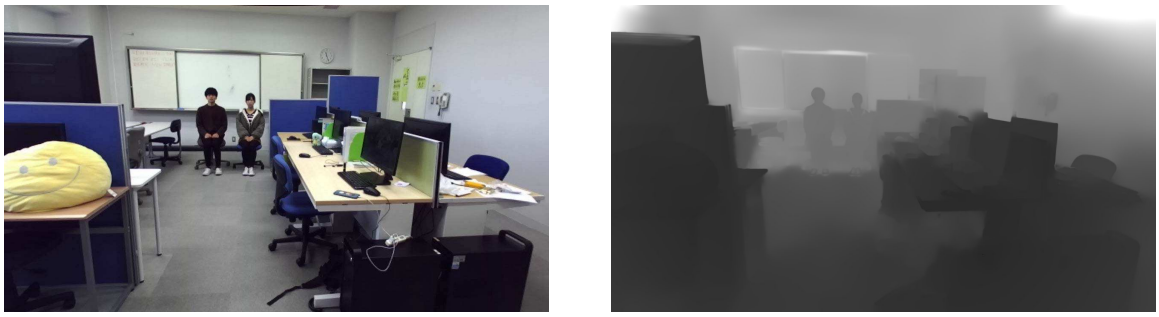

(a) RGB image (b) Depth image

FIGURE 3. RGB-D image (Distant view)

patterns become clearer. On the other hand, when the value of the parameter β becomes small, the shape of photographic images is not preserved and it becomes difficult to recall photographic images from moire-like images. The larger the value of the parameter W, the larger the spacing between moire-like patterns and the more areas where moire-like patterns do not occur. The smaller the value of the parameter T_1, the narrower the spacing between moire-like patterns and the finer curve. The larger the value of the parameter T_2, the clearer moire-like patterns.

3.1. **Experiment changing the value of the parameter γ.** We examined the change in moire-like patterns generated by changing the value of the parameter γ to 0.01, 0.10, 1.00, and 10.00. Moire-like images generated from RGB-D images of Figure 2 and Figure 3 are shown in Figure 4 and Figure 5, respectively. From Figure 4 and Figure 5, it was found that as the value of the parameter γ was larger, moire-like patterns were emphasized and were more distorted. In addition, it was also found that the larger the change in the depth, the greater the distortion of moire-like patterns. The value of the parameter γ may be changed according to the user's preference and usage scene.

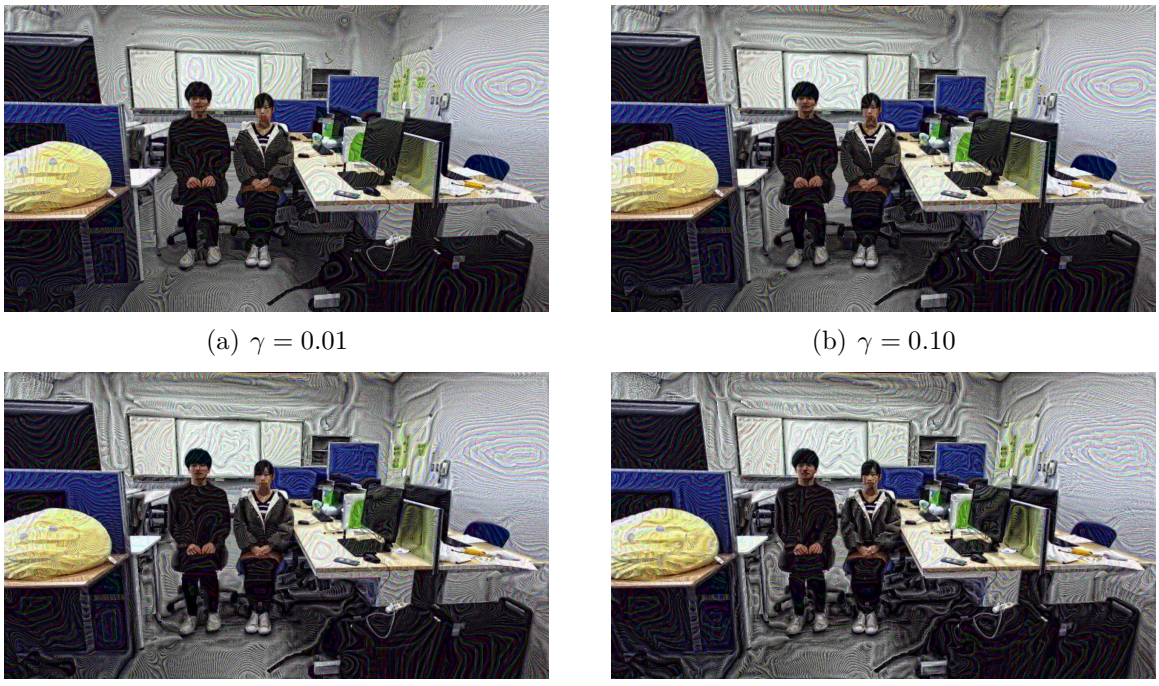

(a) $\gamma = 0.01$ (b) $\gamma = 0.10$

(c) $\gamma = 1.00$ (d) $\gamma = 10.00$

FIGURE 4. Moire-like images (Near view)

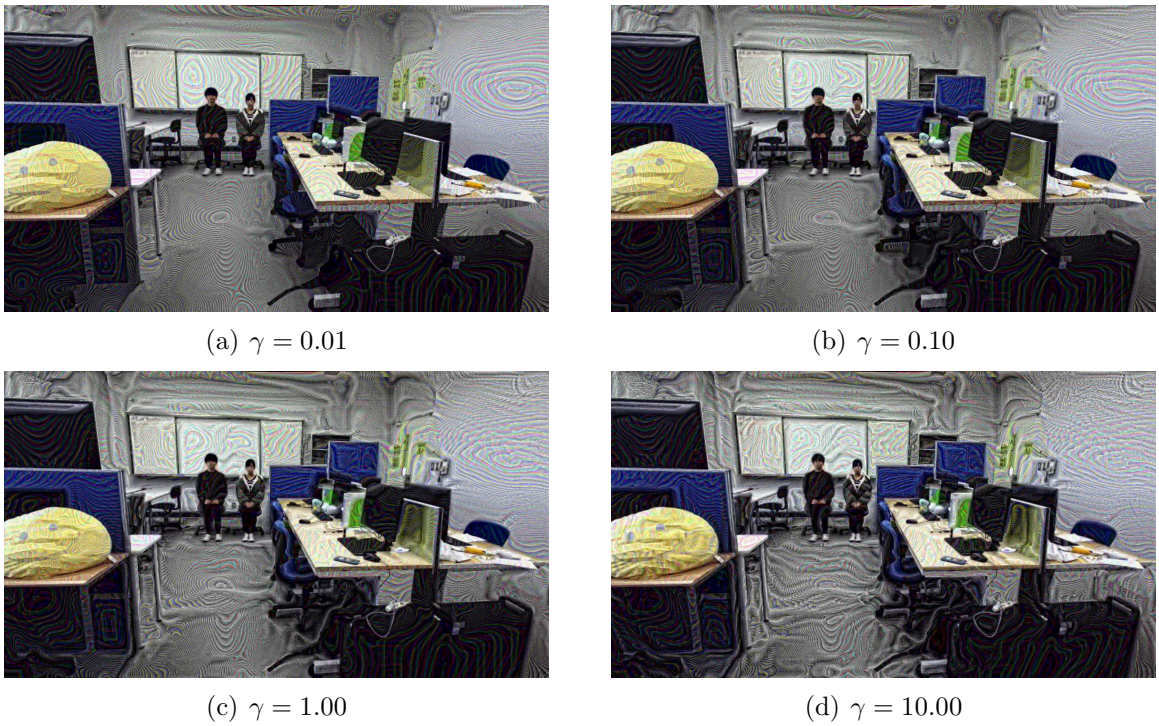

(a) $\gamma = 0.01$ (b) $\gamma = 0.10$

(c) $\gamma = 1.00$ (d) $\gamma = 10.00$

FIGURE 5. Moire-like images (Distant view)

3.2. **Comparison experiment with the conventional method.** We visually compared moire-like images of the proposed and conventional methods. Moire-like images generated from RGB images of Figure 2 and Figure 3 by the conventional method are shown in Figure 6. From Figure 4, Figure 5, and Figure 6, it was found that moire-like images of the proposed method were expressed in more distorted moire-like patterns than moire-like images of the conventional method. In addition, it was also found that moire-like patterns of the conventional method were slightly angular, but moire-like patterns of the proposed method were expressed more smoothly.

(a) Near view (b) Distant view

FIGURE 6. Moire-like images of the conventional method

4. **Conclusions.** We proposed a method for changing the shape of moire-like patterns in moire-like images by using RGB-D images. The proposed method added the depth to the coefficient of bilateral filter. To verify the effectiveness of the proposed method, we performed experiments using RGB-D images obtained by the stereo camera. As this time, we visually examined the change in moire-like patterns generated by changing the value of the parameter newly added by the proposed method. As a result of the experiments, it was found that spatial distortion can be adjusted by changing the value of the parameter.

In addition, it was found that moire-like images different from the conventional method with more distorted moire-like patterns can be generated.

The future task is to apply the proposed method to more RGB-D images, although this paper applied the proposed method to two types of RGB-D images.

Acknowledgment. This work was supported by JSPS KAKENHI Grant Number JP19K 12664.

REFERENCES

[1] C. Tomasi and R. Manduchi, Bilateral filtering for gray and color images, *Proc. of ICCV*, pp.839-846, 1998.

[2] S. Paris, P. Kornprobst, J. Tumblin and F. Durand, Bilateral filtering: Theory and applications, *Foundations and Trends in Computer Graphics and Vision*, vol.4, no.1, pp.1-73, 2008.

[3] R. Matsumura and A. Hanazawa, Human detection using color contrast-based histograms of oriented gradients, *International Journal of Innovative Computing, Information and Control*, vol.15, no.4, pp.1211-1222, 2019.

[4] H. Yang, W. Gan, F. Chen and X. Li, Face recognition using shearlets edges fusion, *International Journal of Innovative Computing, Information and Control*, vol.15, no.4, pp.1309-1322, 2019.

[5] C. Lee and B.-D. Lee, Enhancement for automatic extraction of RoIs for bone age assessment based on deep neural networks, *ICIC Express Letters*, vol.14, no.2, pp.163-170, 2020.

[6] B. Xu, G. Liu and Y. Dai, Robust method for photorealistic computer graphics forensics, *ICIC Express Letters*, vol.8, no.7, pp.1827-1831, 2014.

[7] L. Xue, X. Yi, Y.-C. Lin and J. W. Drukker, An approach of the product form design based on gra-fuzzy logic model: A case study of train seats, *International Journal of Innovative Computing, Information and Control*, vol.15, no.1, pp.261-274, 2019.

[8] A. Buades, B. Coll and J.-M. Morel, The staircasing effect in neighborhood filters and its solution, *IEEE Trans. Image Processing*, vol.15, no.6, pp.1499-1505, 2006.

[9] N. Pierazzo and G. Facciolo, Data adaptive dual domain denoising: A method to boost state of the art denoising algorithms, *Image Processing on Line*, vol.7, pp.93-114, 2017.

[10] T. Hiraoka and K. Urahama, Generation of moire-picture-like color images by bilateral filter, *IEICE Trans. Information and Systems*, vol.E96-D, no.8, pp.1862-1866, 2013.

[11] T. Hiraoka, H. Nonaka and E. C. A. Carreon, Reduction of iterative calculation and quality improvement for generation of moire-like images using bilateral filter, *ICIC Express Letters*, vol.13, no.10, pp.949-954, 2019.

[12] T. Hiraoka and H. Nonaka, Method for moving moire patterns on moire-like images, *ICIC Express Letters*, vol.11, no.10, pp.1533-1538, 2017.

[13] T. Hiraoka and K. Urahama, Moire-like images using binarized-weight bilateral filter for higher quality and speed, *ICIC Express Letters*, vol.11, no.11, pp.1685-1690, 2017.